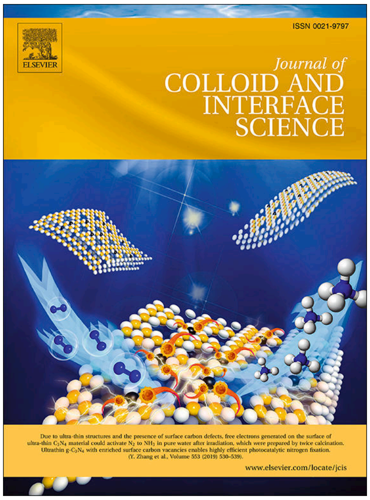

Photoluminescence and Photo-induced conductivity in 2D Siloxene Nanosheet for optoelectronic applications

Supriya Mondal, Tapas Kumar Mondal, Yan-Kuin Su, Shyamal K. Saha

PII: S0021-9797(19)31423-7
DOI: https://doi.org/10.1016/j.jcis.2019.11.095
Reference: YJCIS 25712

To appear in: *Journal of Colloid and Interface Science*

Received Date: 30 August 2019
Revised Date: 18 November 2019
Accepted Date: 23 November 2019

Please cite this article as: S. Mondal, T. Kumar Mondal, Y-K. Su, S.K. Saha, Photoluminescence and Photo-induced conductivity in 2D Siloxene Nanosheet for optoelectronic applications, *Journal of Colloid and Interface Science* (2019), doi: https://doi.org/10.1016/j.jcis.2019.11.095

Photoluminescence and Photo-induced conductivity in 2D Siloxene Nanosheet for optoelectronic applications

Supriya Mondal[a, b], Tapas Kumar Mondal[a] Yan-Kuin Su[c] and Shyamal K. Saha[a, *]

[a]School of Materials Sciences, Indian Association for the Cultivation of Science, Jadavpur, Kolkata, 700032, India

[b]Department of Physics, Government General Degree College, Chapra

Shikra, Padmamala, Nadia, 741123, India

[c]Green Energy Technology Research Center , Kun Shan University, Tainan, Taiwan (R.O.C)

Email of corresponding author: *cnssks@iacs.*res.*in

Abstract:

Semiconducting 2D siloxene nanosheets of thickness 1.7nm and band gap of 2.54 eV are synthesized using simple chemical route. Strong photoluminescence is observed in the as-synthesized nanosheets due to presence of oxygen atoms. The photoluminescence behaviour of siloxene nanosheets is investigated by controlling temperature, excitation and pH of the solution to understand the optical response and stability of the material. The as-synthesized sample heated with temperature 200℃ shows a blue shift of 90 nm compared to the sample synthesized at room temperature. The low temperature luminescence measurements of as-synthesized samples dried at different temperatures viz. 27, 100 and 200℃. It is seen that the luminescence intensity is increasing with decreasing temperature for the sample dried at room temperature. However, after heating the sample at 100℃, the luminescence intensity is not only increased but also red-shifted up to 52 nm. The photocurrent has been measured for the device structure of ITO/PEDOT: PSS/Siloxene/Al with different film thicknesses to optimize the photocurrent and the maximum percentage change in photo power gain. The maximum photopower gain of 2693% is observed for the film thickness of 600nm.

Keywords: Siloxene Nanosheet, Rapidly synthesized, Photoluminescence, Photo-induced conductivity

1. Introduction

Now-a-days, the two-dimensional (2D) materials are the main focus in the area of nanoscale materials because of their unique structures, electronic and optical properties and applications in nano devices. Extensive research has been carried out on graphene, the two-dimensional (2D) hexagonal lattice in different field's viz. field effect transistors [1-4], organic photovoltaic [5-7] and transparent conducting coating for optoelectronic devices [8-13]. It is well known that graphene has a very poor optical activity because of its zero band gap. However, superior optical property has been generated in graphene by introducing functionalization, doping or intercalation [14-25] techniques. On the other hand, siloxene, another graphene like 2D material with silicon backbone is a direct band gap semiconductor. Therefore, siloxene is an alternative 2D material which possesses good optical activity without any functionalization, doping or intercalation. Different chemical structures such as Weiss structure and the Kautsky structure are already available in the literature [26-28]. Deak et al. presented the oxygen incorporation into a planar silicon matrix resulting quantum confinement effect which is responsible for the luminescence behaviour [29]. Here we have introduced a simple technique to synthesize siloxene nanosheets. The two-dimensional (2D) silicon network in siloxene is characterized via XRD, FTIR, TEM, XPS, UV-Vis absorption etc. The direct band gap (2.54 eV) of siloxene also demands the pronounced upcoming 2D semiconductor for application in electronic devices. The photoluminescence of siloxene nanosheets is investigated carefully with respect to excitation, temperature, and pH effect to understand the optical response and stability of the material. The temperature dependent PL spectra of siloxene nanosheets are carried out for the excitation at 380 nm. The intensity of photoluminescence of 2D siloxene nanosheet is increased significantly with decreasing temperature down to 120K. Upon further decreasing the temperature down to 77K, the

PL intensity becomes almost saturated. From the pH dependent PL spectra it is seen that the maximum intensity is obtained at pH 1 and the intensity is gradually decreasing and blue shifted with increasing pH from 1 to 10. The PL spectra of sample heated at different temperatures (27-200℃) are measured. The low temperature PL measurements for the siloxene heated at different temperatures 100 and 200℃ in the form of film are carried out over the temperature from 77-300K. It is seen that the PL intensity is increased for sample heated at 200℃ whereas for sample heated at 100℃ the PL intensity not only increased but also red-shifted by an amount of 52nm. The decay time (1.38ns) of exciton has been measured carefully to investigate the change in electronic conductivity under light i.e. photoconductivity. So, the photocurrent has been measured for the device structure of ITO/PEDOT: PSS/Siloxene/Al. We have also measured the change in photocurrent for different thicknesses of siloxene nanosheets. It is to be mentioned that noticeable power gain (**$\Delta P/P_D$**=2693%) is achieved for the as-synthesized siloxene film of thickness of 600nm.

2. Experimental section

2.1. Materials: Calcium silicide ($CaSi_2$, Merck), hydrochloric acid (35%, Merck), ethanol (99.9%, Merck), indium tin oxide (ITO) coated glass and double distilled water were used as received.

2.2. Synthesis of siloxene sheet from $CaSi_2$:

A mixture of 0.5g of $CaSi_2$ in 20ml conc. HCl (35%) is dispersed at 0^0 C and sonicated for 2h. After sonication the black residue is turned to yellowish green and then it is poured in to 100ml of ethanol taken in a beaker. This material was washed several times using ethanol to remove $CaCl_2$ and dried in vacuum oven at 50^0 C.

$$3CaSi_2+6HCl+3H_2O= Si_6H_3(OH)_3+3CaCl_2+3H_2$$

2.3. Characterization:

Fourier Transform Infra-Red (FTIR) measurements are carried out using a NICOLET MAGNA IR 750 system. Raman spectra of the composites are done using a micro-Raman JYT-6400 model. The crystal structure of the sample is determined by a X-ray diffractometer (Seifert 3000P) using Cu Kα radiation (λ = 1.54178 Å). The morphology and the detailed structural features are investigated by a high-resolution transmission electron microscopy (HRTEM; JEOL 2100). UV-Vis measurements are taken with a Cary UV 5000 spectrophotometer. Photoluminescence spectra are collected using PTI QM-400 spectroflurometer. The optical measurements were done by taking a small amount of the purified sample dispersed in ethanol in a quartz cuvette for pH dependent spectra. The fabrication of the device is provided in the **Fig. S1** (Supporting Information). In the first step, ITO (indium tin oxide) coated glass is properly cleaned through ultrasonic vibration in acetone and isopropyl alcohol and dried it in a dry nitrogen. Then a thin layer of PEDOT: PSS (poly 3, 4-ethylenedioxythiophene: polystyrene sulfonate) is coated on ITO via the spin coater with 5000 rpm and heated in a vacuum oven at 70^0C for 1 h. Siloxene is coated on the PEDOT: PSS layer and dried at room temperature. On the top of the Siloxene film an Al electrode of thickness ~ 100 nm is deposited using a thermal evaporator and the photocurrent is measured in the device structure of ITO/PEDOT: PSS /Siloxene/Al. The Siloxene films of different thicknesses have also been prepared to investigate the thickness dependent photocurrent. Thickness of the film was measured by FE-SEM analysis which is shown in **Fig. S2** (supporting Information). The current-Voltage (I-V) measurements are carried out with the electrometer at room temperature. An electrometer (Keithley 2601) is connected to the two electrodes of the device. Photocurrent measurements are performed under the UV irradiation (365nm) using Xenon lamp.

3. Results and Discussion

3.1. Morphology and structural study: The FTIR measurement has been performed to measure the different vibrational modes of siloxene. **Fig.1a** shows the peaks according to the respective vibrational modes. A broad absorption peak at 3460cm^{-1} corresponds to O-H stretching vibration for siloxene synthesized at room temperature. Two peaks with very small intensities at 2245 cm^{-1} and 2134cm^{-1} correspond to H-SiO_3 and Si-H stretching vibrations [30]. The Peak for O-H bending vibration is appeared at 1623cm^{-1}. A very sharp peak arises at 1067cm^{-1} due to Si-O-Si stretching vibration. Peak at 873cm^{-1} appears for Si-H_2 scissor mode. Peaks at 938 cm^{-1} and 446cm^{-1} are ascribed to Si-O-Si bend stretching and Si-O-Si bending vibration [31] respectively. We have also measured the FTIR spectra of the siloxene annealed at 100 ^{0}C and 200 ^{0}C. The broad absorption peak at 3460cm^{-1} is decreased in case of annealed samples indicating the removal of –OH groups from the siloxene. We have also studied the Raman spectra for potential conformation of Si-O-Si in siloxene. Normally, the strong Raman peak of Si-O-Si arises in the region 450-550 cm^{-1}. The experimental result of **Fig.1b** shows the peak at 517 cm^{-1} due to the motion of O in Si-O-Si symmetric stretching-bending modes.

To investigate the morphology and structure of Siloxene, we have measured the high-resolution transmission electron microscopy (TEM) and X-ray diffraction (XRD) respectively. The X-ray diffraction pattern of as-prepared siloxene is shown in **Fig. 2**a. The diffraction peaks observed at 14.1° and 26.1° correspond to the (001) and (100) planes of two-dimensional (2D) silicon derived from $CaSi_2$ with a hexagonal unit cell [32]. The broad peak at $2\theta=14.1°$ represents the siloxene interlayer spacing confirming the layer type structure of siloxene. The lower magnified TEM images in **Fig. 2b** show almost layer type structure of Siloxene and EDX analysis of the TEM image represents the presence of Si and O in siloxene as given in **Fig. S3** (Supporting Information). We have also measured atomic force microscopy (AFM) to characterize the thickness and surface morphology. Here we observe the 2D sheet of thickness 1.7nm as shown in **Fig. 3.** Therefore, AFM images confirm the formation of 2D nanosheet of siloxene.

3.2 Optical and photoconductivity study

3.2.1 UV-Vis study:

The UV-Vis absorption spectra of siloxene at room temperature are shown in **Fig. 4**a. Two peaks are observed, one being due to $\pi-\pi^*$transition at 240nm and the other due to $n-\pi^*$transition at 400nm. The optical band gap of siloxene has been determined from the absorption spectra. The absorption occurs due to interband transition among extended states in both valence and conduction bands. The absorption coefficient depends on optical band gap, given by:

$$\alpha(\nu)= K(h\nu - E_g)^n/h\nu \qquad (1)$$

where E_g represents the optical band gap, K is a constant and n depends on the nature of the transition having values of 1/2, 3/2, 2, and 3 for allowed direct transitions, forbidden direct transitions, allowed indirect transitions, and forbidden indirect transitions respectively. The siloxene shows the direct band gap of 2.54 eV which is quite interesting result due to the growth of two dimensional arrays of Si and O atoms. The theoretical calculation of siloxene represents the direct band gap of the order of 1.5 eV to 2.7 eV [33-34].

3.2.2 Photoluminescence (PL) Study: Photoluminescence (PL) is a non-destructive and powerful method to investigate the carrier recombination and transport characteristics in semiconductor materials. Here we have measured the excitation, temperature and pH dependent photoluminescence of siloxene as shown in **Fig. 5**. From the excitation dependent PL, we have shown that the recombination occurs at a particular luminescent centre for the wide range of excitation from 300nm to 520nm as shown in **Fig. 5a**. The maximum PL intensity is obtained at room temperature for the excitation of 380nm.

The pH dependent PL of siloxene is studied to understand the influence of surface functional groups on the fluorescence of siloxene. The luminescence spectra of siloxene are presented as a function of pH which varies from 1 to 10 which is shown in **Fig. 5b**. From the pH dependent PL, we have shown that photoluminescence intensity is the maximum at pH 1 and the intensity is gradually blue shifted and decreased with increasing pH from 1 up to 10 and vanishes the PL property at pH10. This is because of the fact that electrons are donated to the valence band of siloxene form the HOMO of the OH group. Filling up of partial holes by the donating electron should diminish the radiative recombination. So PL is decreased and blue shifted due to the partial filling of upper level of valance band. The mechanism of decreasing PL with increasing pH is schematically shown in **Fig. S4** (Supporting Information).

The temperature dependent PL measurements on the siloxene film are carried out over the temperature range from 77-300K using a low temperature optical cryostat (OXFORD INSTRUMENT- Optistat DN2). **Fig. 5c** shows the PL spectra as a function of temperature at excitation wavelength 380nm. With decreasing temperature down to 120K, the intensity of photoluminescence for the film at room temperature is increased significantly as shown in **Fig 5d**. After further decreasing the temperature down to 77K, the luminosity of the material becomes saturated. This saturation of low-temperature PL mechanism (77 K – 120 K) of the material is dominated by localized PL transitions, while the high-temperature PL mechanism is dominated by the thermal energy which prevents the exciton localization.

We have also measured the PL spectra of siloxene film heated at different temperatures (27 to 200 ℃) as shown in **Fig. 6a** and the PL peak positions at 534, 486, 441, 439 and 439nm are obtained for siloxene film heated at temperatures 27, 50, 100,150 and 200 ℃ respectively. It is observed that the PL peak for the excitation of 380nm is blue shifted with increasing temperature up to 100 ℃ however the PL intensity is reduced with further increasing temperature up to 200℃. It is explained on the basis of the mechanism as shown in **Fig. 7**. We have also investigated the temperature dependent PL spectra for siloxene film heated at different temperatures to understand the luminescence stability. The low temperature PL spectra for the siloxene film heated at temperature 100 and 200℃ are shown in **Fig. 6b & 6c** and it is observed that PL intensity for film heated at 200℃ increases with decreasing temperature but for the film heated at 100℃ the PL intensity is increased as well as peak position is also red shifted up to 52nm. These experiments indicate that the localized states (for –OH groups) in between HOMO and LUMO levels for siloxene heated at 200℃ are almost removed compared to that of the siloxene heated at 100℃.

3.4.3 Time correlated single photon counting (TCSPC) study: Time-Correlated Single Photon Counting (TCSPC) study is performed because of the fact that lifetime measurement is one of the most powerful tools to investigate photoconductivity. The time resolved decay curve of siloxene is shown in **Fig. 6d.** A laser pulse is used as an excitation source of 375 nm to measure the decay times for our sample and the data are best fitted to uniexponential function by using the equation $\langle\tau\rangle = (\Sigma a_i \tau_i^2)/(\Sigma a_i \tau_i)$. The decay time of siloxene sheet is obtained as 1.38ns.

3.2.4 Photoconductivity study: We have studied the change in electronic conductivity of 2D siloxene nanosheet in absence and presence of light using the current- voltage characteristic (I-V). It has been investigated for the device structure of ITO/PEDOT:PSS/Siloxene/Al which is schematically shown in **Fig. S1.** I-V characteristics are measured under the dark and light illumination by xenon source at excitation wavelength of 365nm. The power gain for all the devices are estimated from the I-V curves shown in **Fig. 8** using$\Delta P = \left[\int_{-1.5}^{1.5} Idv\right]_{\text{light}}$ - $\left[\int_{-1.5}^{1.5} Idv\right]_{\text{dark}}$ and are summarized in **Table 1.** The photoconductivity obtained at excitation wavelength of 365nm is shown in **Fig. S5**. It is also seen that the maximum power gain is achieved for the medium thickness (600nm) of siloxene. The thickness dependence of the device performance is also investigated and seen that the photocurrent is the maximum for the sample with medium thickness. For thinner sample, a portion of light passes through the film resulting lower photocurrent while for thicker sample increased scattering from the extra layers reduces the photocurrent. Therefore, the optimum film thickness for the best device performance is 600nm.

4. Conclusion:

In summary, it is seen that graphene being a very good 2D electronic material, its optical property is very poor due to its zero gap. Its optical property has been generated by introducing functionalization, doping or intercalation [13-24, 34] techniques. However, in the present work, we have introduced another graphene like two dimensional mateial with silicon backbone i.e. siloxene nanosheet, which is a direct bandgap semiconductor synthesized using a very simple route. It takes only 2 hours to synthesize. The photoluminescence behaviour of 2D semiconductor siloxene with direct band gap has been successfully characterized in details with respect to excitation, pH and heating effect to understand the luminescence intensity, photostability. From the photo response of the material with respect to excitation, heating effect and pH effect it is seen that the 2D siloxene nanosheet which does not need any functionalization, doping or intercalation to synthesize as compared to graphene might be an alternative for the upcoming semiconductor industry for application in electronic devices.

ASSOCIATED CONTENT

Supporting Information

FE-SEM image, EDX analysis of siloxene nanosheet, schematic diagram of the device, mechanism of pH dependent PL and photoconductivity for siloxene nanosheet are given in Supporting Information

AUTHOR INFORMATION

Corresponding Author *E-mail: cnssks@iacs.res.in.

Notes

The authors declare no competing financial interest.

ACKNOWLEDGMENTS

S. M. acknowledges Government General Degree College at Chapra, Shikra, Padmamala, Nadia, Govt. of West Bengal for giving permission to continue PhD work, T.K.M. acknowledges CSIR, New Delhi for awarding fellowships. SKS acknowledges DST, New Delhi, Govt. of India for infrastructural facilities.

Reference:

[1] S. W. Hong, F. Du, W. Lan, S. Kim, H. S. Kim, J. A. Rogers, Monolithic Integration of Arrays of Single-Walled Carbon Nanotubes and Sheets of Graphene, Adv. Mater. 23 (**2011**) 3821-3826.

[2] B. Li, X. Cao, H. G. Ong, J. W. Cheah, X. Zhou, Z. Yin, H. Li et al., All-Carbon Electronic Devices Fabricated by Directly Grown Single-Walled Carbon Nanotubes on Reduced Graphene Oxide Electrodes, Adv. Mater. 22 (**2010**) 3058-3061.

[3] L. Liao, Y. C. Lin, M. Bao, R. Cheng, J. Bai, Y. Liu, Y. Qu, K. L. Wang, Y. Huang, X. Duan, High-speed graphene transistors with a self-aligned nanowire gate, Nature 467 (**2010**) 305.

[4] C. Di, D. Wei, G. Yu, Y. Liu, Y. Guo, D. Zhu, Patterned graphene as source/drain electrodes for bottom-contact organic field-effect transistors, Adv. Mater. 20 (**2008**) 3289-3293.

[5] T. H. Han, Y. Lee, M. R. Choi, S. H. Woo, S. H. Bae, B. H. Hong, J. H. Ahn, T. W. Lee, Extremely efficient flexible organic light-emitting diodes with modified graphene anode, Nat. Photonics 6 (**2012**) 105.

[6] J. R. Sheats, H. Antoniadis, M. Hueschen, W. Leonard, J. Miller, R. Moon, D. Roitman, A. Stocking, Organic electroluminescent devices, Science 273 (**1996**) 884-888.

[7] X. Huang, Z. Zeng, Z. Fan, J. Liu, H.Zhang, Graphene-based electrodes, Adv. Mater. 24 (**2012**) 5979-6004.

[8] K. Rana, J. Singh, J. H. Ahn, A graphene-based transparent electrode for use in flexible optoelectronic devices, J. Mater. Chem. C 2 (**2014**) 2646-2656.

[9] Z. Liu, Q. Liu, Y. Huang, Y. Ma, S. Yin, X. Zhang, W. Sun, Y. Chen, Organic photovoltaic devices based on a novel acceptor material: graphene, Adv. Mater. 20 (**2008**) 3924-3930.

[10] Y. D. Kim, H. Kim, Y. Cho, J. H. Ryoo, C. H. Park, P. Kim, Y. S. Kim et al. Bright visible light emission from graphene, Nat. Nanotechnol. 10 (**2015**) 676.

[11] S. Mondal, S. Sudhu, S. Bhattacharya, S.K. Saha, Strain-induced tunable band gap and morphology-dependent photocurrent in RGO–CdS nanostructures, J. Phys. Chem. C 119 (**2015**) 27749-27758.

[12] S. Mondal, D. Dinda, B. K. Shaw, S. K. Saha, Tunable color in 2, 6-diaminopyridine-functionalized graphene oxide, J. Phys. Chem. C 120 (**2016**) 11085-11091.

[13] Fang Pan, Zhiming Lu, Ian Tucker, Sarah Hosking, Jordan Petkov, Jian R. Lu, Surface active complexes formed between keratin polypeptides and ionic surfactants, Journal of Colloid and Interface Science, 484, (2016), 125-134

[14] Z. Qian, J. Zhou, J. Chen, C. Wang, C. Chen, H.Feng, Nanosized N-doped graphene oxide with visible fluorescence in water for metal ion sensing, J. Mater. Chem. 21 (**2011**) 17635-17637.

[15] Y.Li, Y. Zhao, H. Cheng, Y. Hu, G. Shi, L. Dai, L.Qu, Nitrogen-doped graphene quantum dots with oxygen-rich functional groups, J. Am. Chem. Soc. 134 (**2011**) 15-18.

[16] D. Dinda, A. Gupta, B. K. Shaw, S. Sadhu, S. K. Saha, Highly selective detection of trinitrophenol by luminescent functionalized reduced graphene oxide through FRET mechanism, ACS Appl. Mater. Interfaces 6 (**2014**) 10722-10728.

[17] Y.Xu, H. Bai, G. Lu, C. Li, G. Shi, Flexible graphene films via the filtration of water-soluble noncovalent functionalized graphene sheets, J. Am. Chem. Soc. 130 (**2008**) 5856-5857.

[18] C. T.Chien, S. S. Li, W. J. Lai, Y. C.Yeh, H. A. Chen, I. S. Chen, L. C. Chen et al., Tunable photoluminescence from graphene oxide, Angew. Chem. 51 (**2012**) 6662-6666.

[19] Z. X.Gan, S. J. Xiong, X. L. Wu, C. Y. He, J. C. Shen, P. K. Chu, Mn^{2+}-bonded reduced graphene oxide with strong radiative recombination in broad visible range caused by resonant energy transfer, Nano Lett. 11 (**2011**) 3951-3956.

[20] Y. Xu, Z. Liu, X. Zhang, Y. Wang, J. Tian, Y. Huang, Y. Ma, X. Zhang, Y. Chen, A graphene hybrid material covalently functionalized with porphyrin: synthesis and optical limiting property, Adv. Mater. 21 (**2009**) 1275-1279.

[21] K. P. Loh, Q. Bao, G. Eda, M. Chhowalla, Graphene oxide as a chemically tunable platform for optical applications, Nat. Chem. 2 (**2010**) 1015.

[22] B. K. Gupta, P. Thanikaivelan, T. N. Narayanan, L. Song, W. Gao, T. Hayashi, A. L. M. Reddy et al., Optical bifunctionality of europium-complexed luminescent graphene nanosheets, Nano Lett. 11 (**2011**) 5227-5233.

[23] S. Mondal, A. Gupta, B. K. Shaw, S. K. Saha, Photo-induced conductivity in 2, 6-diaminopyridine functionalized graphene oxide containing Eu^{2+} for optoelectronic applications, Opt. Mater. 73 (**2017**) 555-562.

[24] J. Wei, Z. Zang , Y. Zhang, M. Wang, J. Du, X. Tang, Enhanced performance of light-controlled conductive switching in hybrid cuprous oxide/reduced graphene oxide (Cu 2 O/rGO) nanocomposites, Opt. Lett. 42 (**2017**) 911-914.

[25] T. K. Mondal, A. Gupta, B. K. Shaw, S. Mondal, U. K. Ghorai, S. K. Saha, Highly luminescent N-doped carbon quantum dots from lemon juice with porphyrin-like structures surrounded by graphitic network for sensing applications, RSC Adv. 6 (**2016**) 59927-59934.

[26] S. Yamanaka, H. Matsu-ura, M. Ishikawa, New deintercalation reaction of calcium from calcium disilicide. Synthesis of layered polysilane, Mater. Res. Bull.31 (**1996**) 307-316.

[27] J. R. Dahn, B. M. Way, E. Fuller, J. S. Tse, Structure of siloxene and layered polysilane (Si_6 H_6), Phys. Rev. B 48 (**1993**) 17872.

[28] H. Oughaddou, H. Enriquez, M. R. Tchalala, H. Yildirim, A. J. Mayne, A. Bendounan, G. Dujardin, M. A. Ali, A. Kara, Silicene, a promising new 2D material, Prog. Surf. Sci. 90(**2015**) 46-83.

[29] P. Deak, M. Rosenbauer, M. Stutzmann, J. Weber, M. S. Brandt, Siloxene: Chemical quantum confinement due to oxygen in a silicon matrix, Phys. Rev. Lett. 69 (**1992**) 2531.

[30] A. Molassioti-Dohms, U. Dettlaff-Weglikowska, S. Finkbeiner, W. Hönle, J. Weber, Photo-and Chemiluminescence from Wöhler Siloxenes, J. Electrochem. Soc. 143 (**1996**) 2674-2677.

[31] H. D. Fuchs, M. Stutzmann, M. S. Brandt, M. Rosenbauer, J. Weber, A. Breitschwerdt, P. Deak, M. Cardona, Porous silicon and siloxene: Vibrational and structural properties, Phys. Rev. B48 (**1993**) 8172.

[32] H. Nakano, M. Ishii, H. Nakamura, Preparation and structure of novel siloxene nanosheets, Chem. Comm.23 (**2005**) 2945-2947.

[33] P. Deak, M. Rosenbauer, M. Stutzmann, J. Weber, M. S. Brandt, Siloxene: Chemical quantum confinement due to oxygen in a silicon matrix, Phys. Rev. Lett. 69 (**1992**) 2531.

[34] C. G. Van de Walle, J. E. Northrup, First-principles investigation of visible light emission from silicon-based materials, Phys. Rev. Lett. 70 (**1993**) 1116.

Table 1 The power gain for all the devices are estimated from the I-V curves

Thickness in nm	**Area under the curve (Dark area/Light area)**	**Percentage change in Photo Power Gain ($\Delta P/P_D$)**
Thin film (~230 nm)	P_D=8.948E-5 P_L=9.882E-4	**1004 %**
Medium film (~600nm)	P_D =1.312E-4 P_L =3.66E-3	**2693%**
Thick (>1µm)	P_D =3.468E-2 P_L =8.91E-2	**156%**

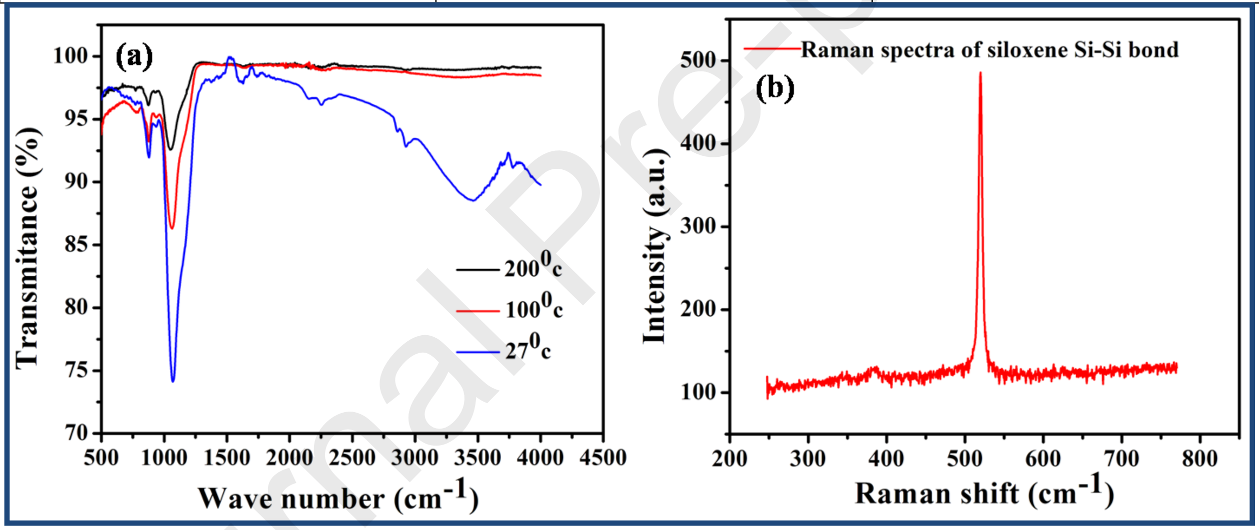

Fig. 1 (a) FT-IR spectra of siloxene; (b) Raman spectra of siloxene

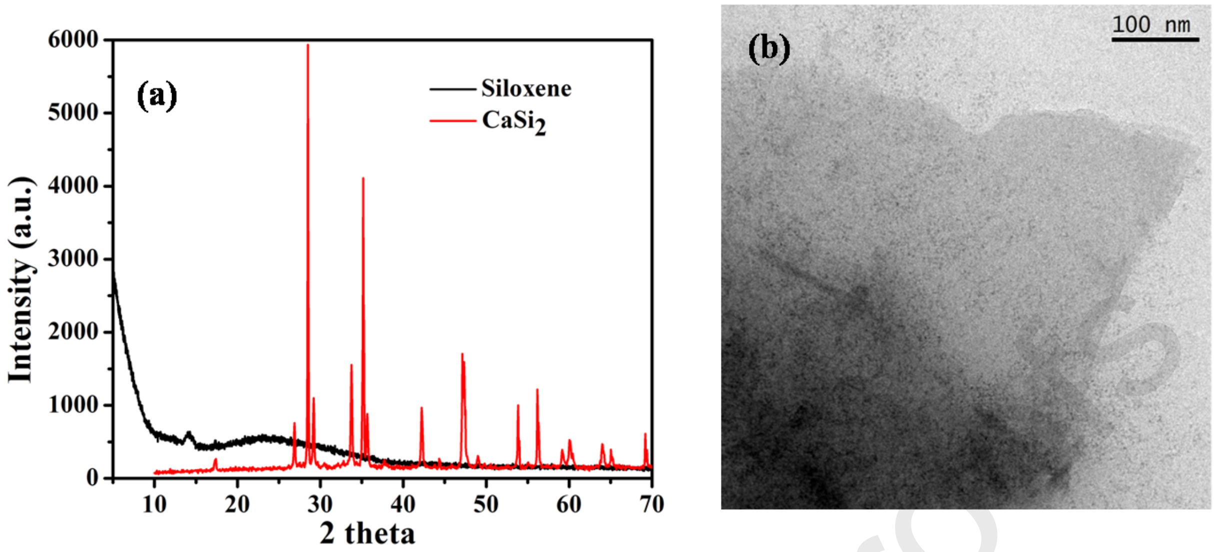

Fig. 2(a) XRD spectra of siloxene; (b) TEMimage of siloxene

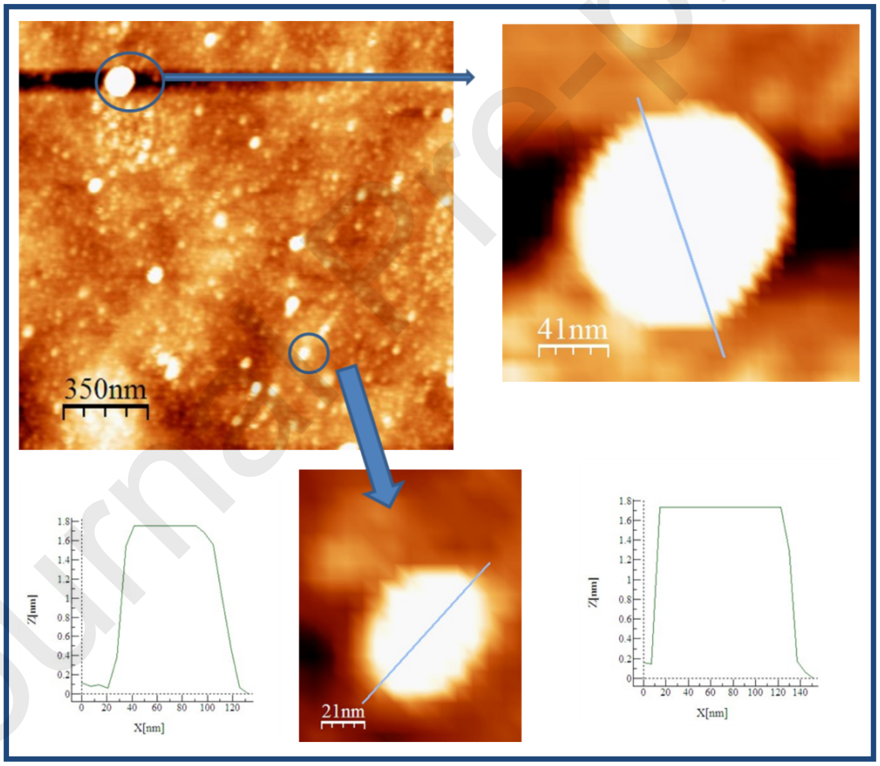

Fig.3 AFM image of siloxene nanosheet

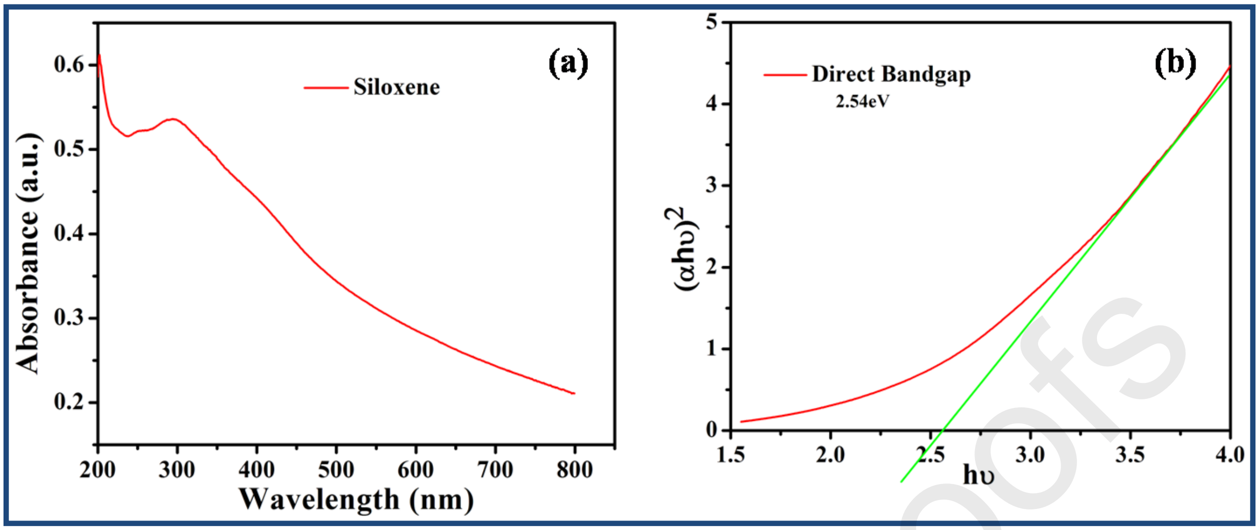

Fig.4 (a) UV-Vis spectra of siloxene nanosheet; (b) direct bandgap of siloxene nanosheet

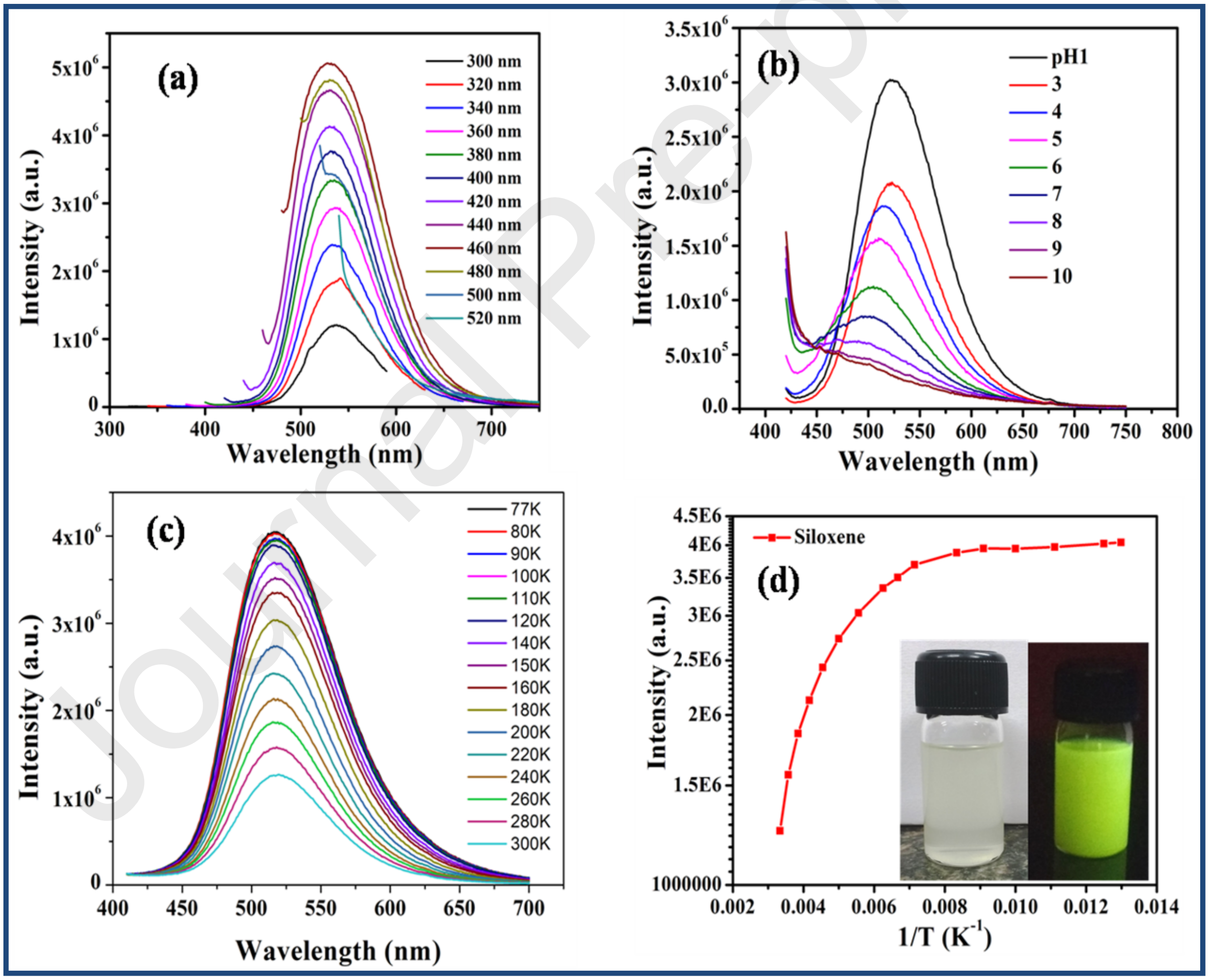

Fig.5 (a) excitation independent photoluminescence spectra of siloxene nanosheet; (b) pH effect on PL spectra of siloxene nanosheet; (c) Low temperature PL spectra of siloxene nanosheet;(d)

PL intensity vs temperature curve of siloxene nanosheet, inset shows digital photograph of siloxene nanosheet under visible and UV light (365nm)

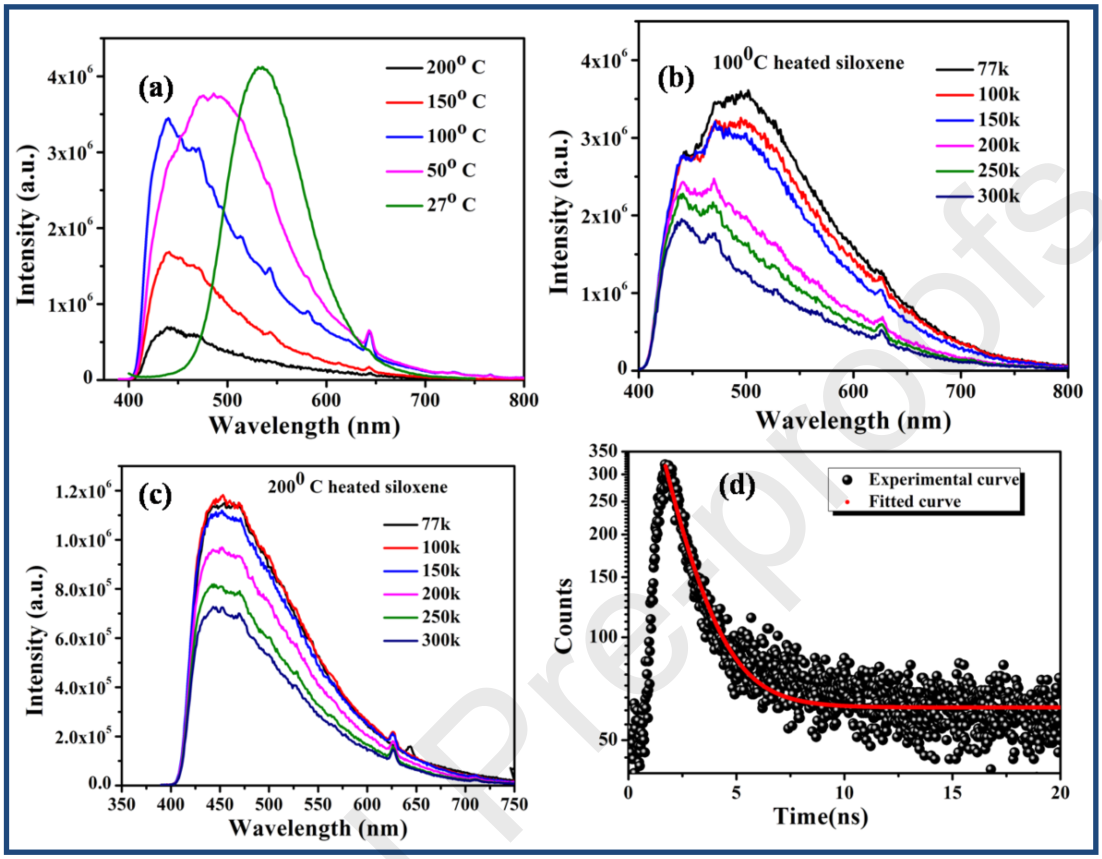

Fig.6 (a) PL spectra of siloxene nanosheet heated at different temperature, The low temperature dependent PL of siloxene heated at (b) 100 ⁰C (c) 200 ⁰C and (d) decay time measurement of siloxene

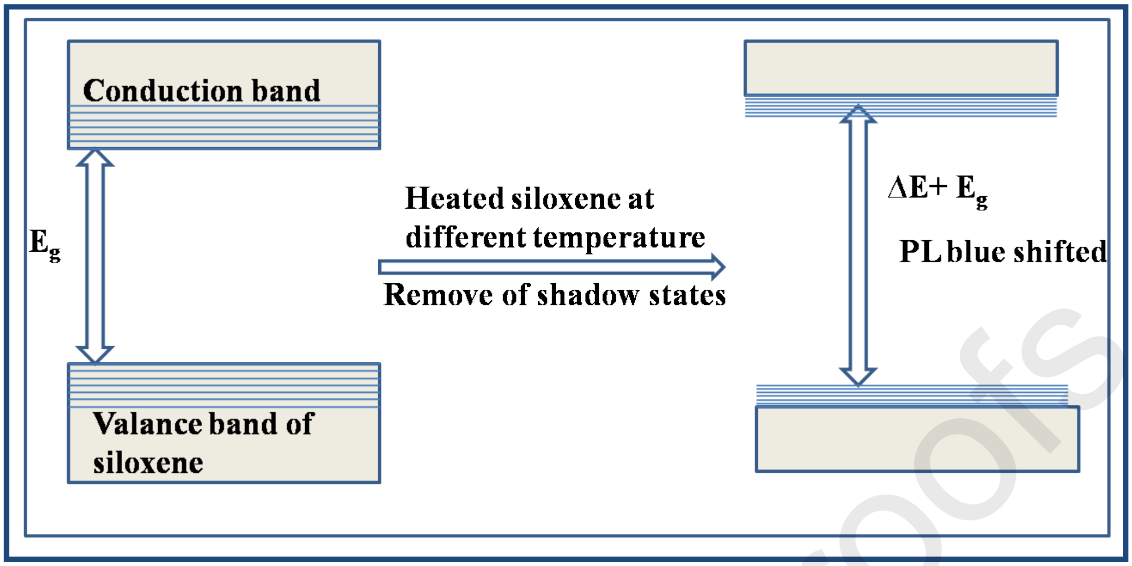

Fig.7 Mechanism of blue shifted PL for heated siloxene nanosheet

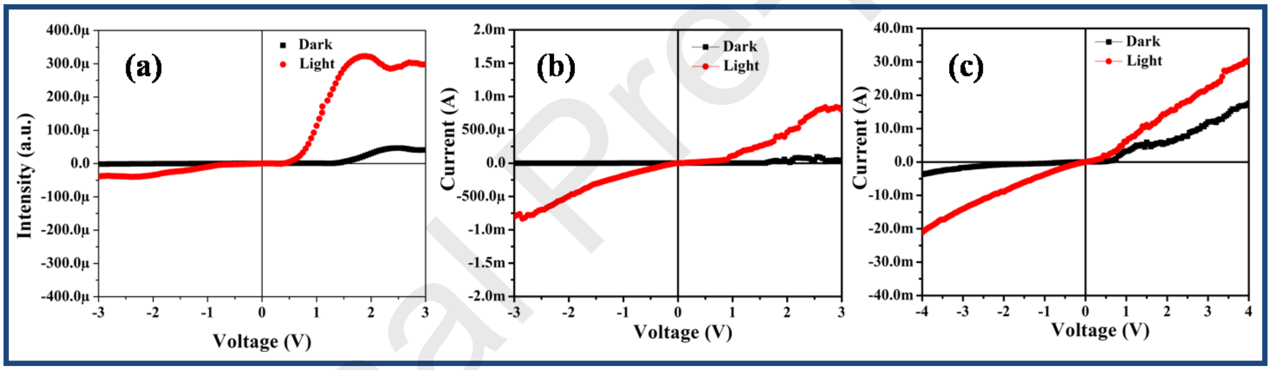

Fig.8. I-V characteristic of siloxene nanosheet for different thickness (a) 230nm (b) 600nm and (c) >1μm

Graphical abstract

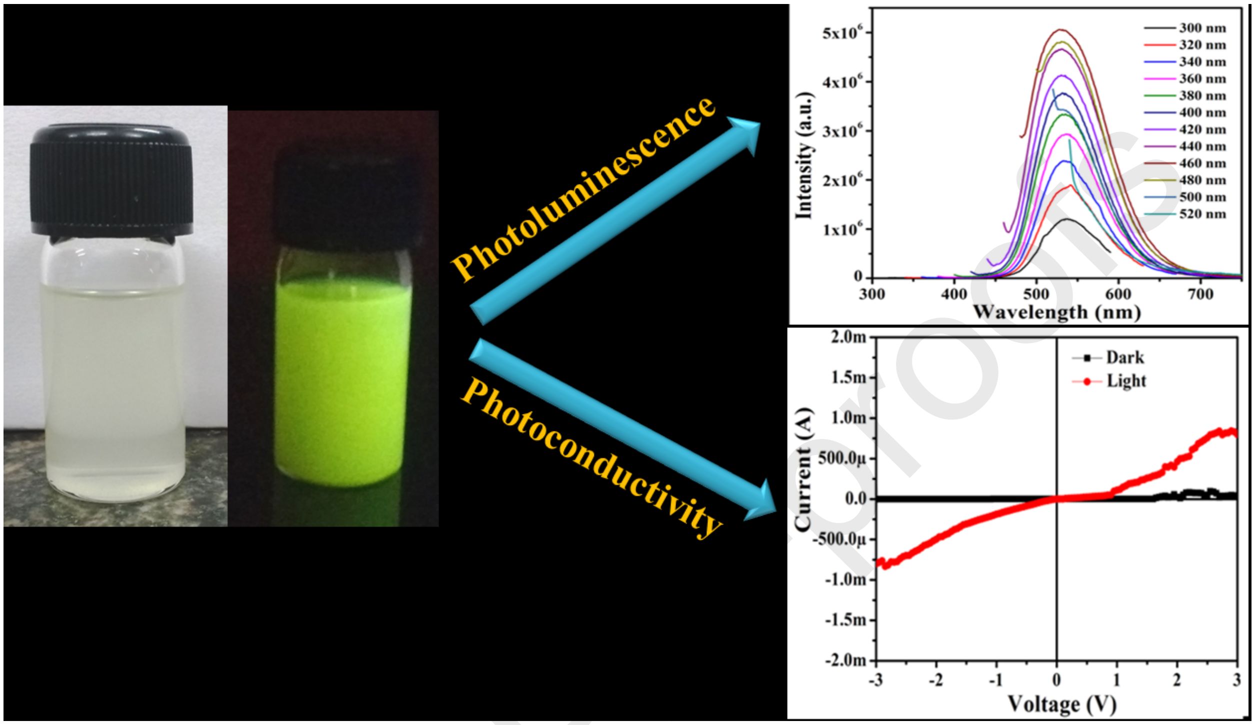

Author's contribution

S. M., T.K.M., Y.K.S. and S.K.S. planned the experiments. S.M. and TKM carried out the experiment. T.K.M. synthesized materials, S.M. fabricated device. S.M. wrote the manuscript with help of T.K.M., Y.K.S. and S.K.S. The project is supervised by S.K.S. All authors discussed the results and contributed to the final manuscript.